

EXHIBIT M

ogy), respectively. Staining specificity was controlled by single staining, as well as by using secondary antibodies in the absence of the primary stain.

Generation of target cells

Target cells displaying a membrane integral version of either wild-type HEL or a mutant¹⁰ exhibiting reduced affinity for HyHEL10 (H2¹⁰, D¹⁰, C¹⁰, H¹⁰) designated HEL¹⁰ were generated by transfecting mouse J5581 plasmacytoma cells with constructs analogous to those used¹⁰ for expression of soluble HEL/H2¹⁰, except that 14 Ser/Gly codons, the H2K¹⁰ transmembrane region, and a 23-codon cytoplasmic domain were inserted immediately upstream of the termination codon by polymerase chain reaction. For mHEL–GFP, we included the EGFP coding domain in the Ser/Gly linker. Abundance of surface HEL was monitored by flow cytometry and radiolabelled antibody binding using HyHEL5 and D1.3 HEL-specific monoclonal antibodies, for which the mutant HELs used in this work show unaltered affinities¹⁰.

Interaction assays

For B-cell/target interaction assays, splenic B cells from 3–83 or MD4 transgenic mice^{18,19} carrying (IgM + IgD) BCRs specific for HEL or H2K¹⁰/H2K¹⁰ were freshly purified on Lympholyse and incubated with a twofold excess of target cells in RPMI, 50 mM HEPES pH7.4, for the appropriate time at 37 °C before being applied to polystyrene-coated slides. Cells were fixed in 4% paraformaldehyde/PBS or methanol and permeabilized with PBS/0.1% Triton X-100 before immunohistochemistry. We acquired confocal images using a Nikon 5800 microscope attached to BioRad Radiance Plus scanning system equipped with 488-nm and 543-nm lasers, as well as different interference contrast for transmitted light. GFP fluorescence in living cells in real time was visualized using a Radiance 2000 and Nikon E300 inverted microscope. Images were processed using BioRad LaserSharp 1024 or 2000 software to provide single plane images, confocal projections or slices.

Antigen presentation

Presentation of HEL epitopes to T-cell hybridomas 2G7 (specific for I-E¹⁰[HEL¹⁰]) and I-E3 (specific for I-E¹⁰[HEL¹⁰]) by transfectants of the LK35.2 B-cell hybridoma expressing an HEL-specific IgM BCR was monitored as described¹⁰.

Received 12 December 2000; accepted 30 March 2001.

1. Lanzavecchia, A. Antigen-specific interaction between T and B cells. *Nature* **314**, 537–539 (1985).
2. Klaus, G. G., Humphrey, J. H., Kishimoto, A. & Doolittle, D. W. The follicular dendritic cells in B cell antigen presentation in the generation of immunological memory. *Immunol. Rev.* **53**, 3–24 (1980).
3. Tew, J. G., Kozes, M. H., Barnes, G. F. & Szalai, A. K. Follicular dendritic cells as accessory cells. *Immunol. Rev.* **117**, 185–211 (1990).
4. Kozes, M. H., Tew, J. G., Schlegel, D. & Julius, M. Follicular dendritic cells help resting B cells to become effective antigen-presenting cells: induction of B7/88 and upregulation of major histocompatibility complex class II molecules. *J. Exp. Med.* **178**, 205–206 (1993).
5. Schamel, W. W. & Barth, M. Monoclonal and oligomeric complexes of the B cell antigen receptor. *Immunol.* **13**, 5–14 (2000).
6. Taylor, R. B., Duffus, W. P. H., Hoff, M. C. & de Petris, S. Redundant and pleiotropic roles of lymphocyte surface immunoglobulin molecules induced by anti-immunoglobulin antibody. *Nature* **235**, 225–227 (1973).
7. Schneider, G. F. & Unanue, E. R. Coupling and the lymphocyte: models for membrane reorganization. *J. Immunol.* **139**, 1549–1551 (1977).
8. Cheng, P. C., Dykstra, M. L., Mitchell, R. N. & Pierce, S. K. A role for lipid rafts in B cell antigen receptor signaling and antigen targeting. *J. Exp. Med.* **190**, 1549–1560 (1999).
9. Weinreich, B. C. et al. Entry of B cell receptor into signaling domains is inhibited in tolerant B cells. *J. Exp. Med.* **191**, 1443–1448 (2000).
10. Bontess, F. D. & Neuberger, M. S. Affinity dependence of the B cell response to antigen: a threshold, a ceiling, and the importance of off rate. *Immunol. Rev.* **75**, 79–109 (1998).
11. Nussenzweig, D. & Burkh, K. Clonal deletion of B lymphocytes in a transgenic mouse bearing anti-MHC class I antibody genes. *Nature* **337**, 560–566 (1989).
12. Hanley, S. B. et al. Elimination from peripheral lymphoid tissues of self-reactive B lymphocytes reorganizing membrane bound antigen. *Nature* **353**, 765–769 (1993).
13. Dustin, M. L. et al. Low affinity interaction of human and rat T cell adhesion molecule CD2 with its ligands allows adhering membranes to achieve high physiological affinity. *J. Biol. Chem.* **273**, 30889–30898 (1998).
14. Lang, J. et al. B cells are exquisitely sensitive to central tolerance and receptor editing by alkaline affinity, membrane bound antigen. *J. Exp. Med.* **184**, 1055–1067 (1996).
15. Valluzzi, S., Muller, S., Colla, M., Padova, E. & Lanzavecchia, A. Serial triggering of many T-cell receptors by a few peptide–MHC complexes. *Nature* **375**, 148–151 (1998).
16. Monks, C. R., Freiberg, B. A., Kupfer, H., Scibelli, N. & Kupfer, A. Three-dimensional aggregation of superantigenic activation clusters in T cells. *Nature* **395**, 82–86 (1998).
17. Wulff, C. & Davis, M. M. A novel mechanism of T cell activation: movement triggered by stimulation during T cell activation. *Science* **282**, 2266–2269 (1998).
18. Grakoui, A. et al. The immunological synapse: a molecular machine controlling T cell activation. *Science* **281**, 221–227 (1999).
19. Levin, O., Zaru, R., Lorsche, T., Muller, S. & Winkler, S. Exclusion of CD45 from the T-cell receptor signaling area in antigen–antibody interactions. *Cell* **103**, 277–289 (2000).
20. Capen, R. L., Kramiec, H., Hart, A. C. & Zipursky, S. L. The balance of seed and seedling interaction: internalization of a transmembrane ligand. *Cell* **69**, 393–399 (1992).
21. Huang, J. F. et al. TCR-mediated internalization of peptide–MHC complexes acquired by T cells. *Science* **286**, 951–954 (1999).
22. Huang, J. F. et al. T cells use either T cell receptor or CD28 receptors to absorb and internalize cell surface molecules derived from antigen-presenting cells. *J. Exp. Med.* **191**, 1137–1148 (2000).
23. Bontess, F. D. & Neuberger, M. S. B cell extrinsic and intrinsic immune responses: implications for affinity discrimination. *EMBO J.* **19**, 513–520 (2000).
24. Casteen, L. A., Lacey, E. K., Jischke, M. L., Margalit, E. & Pierce, S. K. Anti-immunoglobulin

25. suggests the B-cell antigen-presentation function independently of internalization of receptor–antigen complexes. *Proc. Natl Acad. Sci. USA* **82**, 5899–5904 (1985).
26. Srenthos, E., Eickholt, S. J., Williamson, E., Kabata, S. & Clark, M. R. Signals from the B-lymphocyte antigen receptor regulate MHC class II containing late endosomes. *J. Immunol.* **160**, 5203–5208 (1998).
27. Sere, K. et al. Efficient presentation of multivalent antigens targeted to various cell surface molecules of dendritic cells and surface Ig of antigen-specific B cells. *J. Immunol.* **164**, 6859–6867 (1999).
28. Green, S. M., Lowe, A. D., Parnagall, J. & Hart, J. Transformation of growth factor-dependent myeloid stem cells with retroviral vectors carrying c-myc. *Oncogene* **7**, 737–751 (1993).
29. Russell, D. M. et al. Peripheral deletion of self-reactive B cells. *Nature* **334**, 308–311 (1991).
30. Goodnow, C. C. et al. Altered immunoglobulin expression and functional silencing of self-reactive B lymphocytes in transgenic mice. *Nature* **334**, 670–682 (1990).
31. Albrecht, V. R., Eickholt, S. A., Williams, G. T., Adami, L. & Neuberger, M. S. Acceleration of intracellular targeting of antigen by the B-cell antigen receptor: importance depends on the nature of the antigen–antibody interaction. *EMBO J.* **16**, 3553–3561 (1997).

Supplementary information is available on Nature's World Wide Web site (<http://www.nature.com>) or as paper copy from the London editorial office of Nature.

Acknowledgements

We thank B. Amos and S. Reichelt for help and advice with confocal microscopy, and S. Munro for helpful discussions. We are indebted to those who provided antibodies, transgenic mice and cell lines. F.D.B. and D.I. were supported by the Arthritis Research Campaign and Studienstiftung des deutschen Volkes, respectively.

Correspondence and requests for materials should be addressed to E.D.B. (e-mail: fdb@nrc-mbc.cam.ac.uk) or M.S.N. (e-mail: msn@nrc-mbc.cam.ac.uk).

Duplexes of 21-nucleotide RNAs mediate RNA interference in cultured mammalian cells

Sayda M. Elbashir¹, Jens Harborth¹, Wimfried Lendeckel¹, Abdullah Yalcin¹, Klaus Weber² & Thomas Tuschli¹

¹Department of Cellular Biochemistry, and ²Department of Biochemistry and Cell Biology, Max-Planck-Institute for Biophysical Chemistry, Am Fassberg 11, D-37077 Göttingen, Germany

RNA interference (RNAi) is the process of sequence-specific, post-transcriptional gene silencing in animals and plants, initiated by double-stranded RNA (dsRNA) that is homologous in sequence to the silenced gene^{1–4}. The mediators of sequence-specific messenger RNA degradation are 21- and 22-nucleotide small interfering RNAs (siRNAs) generated by ribonuclease III cleavage from longer dsRNAs^{5–9}. Here we show that 21-nucleotide siRNA duplexes specifically suppress expression of endogenous and heterologous genes in different mammalian cell lines, including human embryonic kidney (293) and HeLa cells. Therefore, 21-nucleotide siRNA duplexes provide a new tool for studying gene function in mammalian cells and may eventually be used as gene-specific therapeutics.

Uptake of dsRNA by insect cell lines has previously been shown to 'knock-down' the expression of specific proteins, owing to sequence-specific, dsRNA-mediated mRNA degradation^{10–12}. However, it has not been possible to detect potent and specific RNA interference in commonly used mammalian cell culture systems, including 293 (human embryonic kidney), NIH/3T3 (mouse fibroblast), BHK-21 (Syrian baby hamster kidney), and CHO-K1 (Chinese hamster ovary) cells, applying dsRNA that varies in size between 38 and 1,662 base pairs (bp)^{10,12}. This apparent lack of RNAi in mammalian cell culture was unexpected, because RNAi exists in mouse oocytes and early embryos^{13,14}, and because RNAi-related, transgene-mediated co-suppression was also observed in cultured rat-1 fibroblasts¹⁵. But it is known that dsRNA in the cytoplasm of mammalian cells can trigger profound physiological

reactions that lead to the induction of interferon synthesis¹⁸. In the interferon response, dsRNA > 30 bp binds and activates the protein kinase PKR¹⁷ and 2',5'-oligoadenylate synthetase (2',5'-AS)¹⁸. Activated PKR stalls translation by phosphorylation of the translation initiation factors eIF2 α , and activated 2',5'-AS causes mRNA degradation by 2',5'-oligoadenylate-activated ribonuclease L. These responses are intrinsically sequence-nonspecific to the inducing dsRNA.

Base-paired 21- and 22-nucleotide (nt) siRNAs with overhanging 3' ends mediate efficient sequence-specific mRNA degradation in lysates prepared from *Drosophila* embryos⁸. To test whether siRNAs are also capable of mediating RNAi in cell culture, we synthesized 21-nt siRNA duplexes with symmetric 2-nt 3' overhangs directed against reporter genes coding for sea pansy (*Renilla reniformis*, RL) and two sequence variants of firefly (*Photinus pyralis*, GL2 and GL3) luciferases (Fig. 1a, b). The siRNA duplexes were co-transfected with the reporter plasmid combinations pGL2/pRL or pGL3/pRL, into *Drosophila* S2 cells or mammalian cells using cationic liposomes. Luciferase activities were determined 20 h after transfection. In *Drosophila* S2 cells (Fig. 2a and b), the specific inhibition of luciferases was complete and similar to results previously obtained for longer dsRNAs^{8,19,9}. In mammalian cells, where the reporter genes were 50- to 100-fold more strongly expressed, the specific suppression was less complete (Fig. 2c-j). In NIH/3T3, monkey COS-7 and HeLa S3 cells (Fig. 2c-h), GL2 expression was reduced 3-

to 12-fold, GL3 expression 9- to 25-fold, and RL expression 2- to 3-fold, in response to the cognate siRNAs. For 293 cells, targeting of RL luciferase by RL siRNAs was ineffective, although GL2 and GL3 targets responded specifically (Fig. 2i and j). The lack of reduction of RL expression in 293 cells may be because of its expression, 5- to 20-fold higher than any other mammalian cell line tested and/or to limited accessibility of the target sequence due to RNA secondary structure or associated proteins. Nevertheless, specific targeting of GL2 and GL3 luciferase by the cognate siRNA duplexes indicated that RNAi is also functioning in 293 cells.

The 2-nucleotide 3' overhang in all siRNA duplexes was composed of (2'-deoxy) thymidine, except for uGL2, which contained

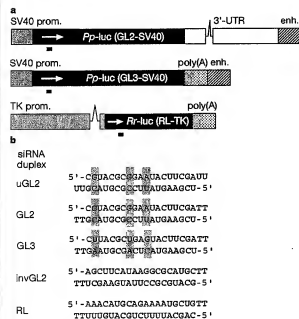


Figure 1 Reporter constructs and siRNA duplexes. **a**, The firefly (*Pp-luc*) and sea pansy (*Rl-luc*) luciferase reporter-gene regions from plasmids pGL2-Control, pGL3-Control, and pRL-TK (Promega) are illustrated; simian virus 40 (SV40) promoter (prom.); SV40 enhancer element (enh.); SV40 late polyadenylation signal (polyA); herpes simplex virus (HSV) thymidine kinase promoter, and two introns (lines) are indicated. The sequence of GL3 luciferase is 95% identical to GL2, but RL is completely unrelated to both. Luciferase expression from pGL2 is approximately 10-fold lower than from pGL3 in transfected mammalian cells. The region targeted by the siRNA duplexes is indicated as black bar below the coding region of the luciferase genes. **b**, The sense (top) and antisense (bottom) sequences of the siRNA duplexes targeting GL2, GL3, and RL luciferases are shown. The GL2 and GL3 siRNA duplexes differ by only three single-nucleotide substitutions (boxed in grey). As nonspecific control, a duplex with the inverted GL2 sequence, InvGL2, was synthesized. The 2-nucleotide 3' overhang of 2'-deoxythymine is indicated as TT; uGL2 is similar to GL2 siRNA but contains ribo-uridine 3' overhangs.

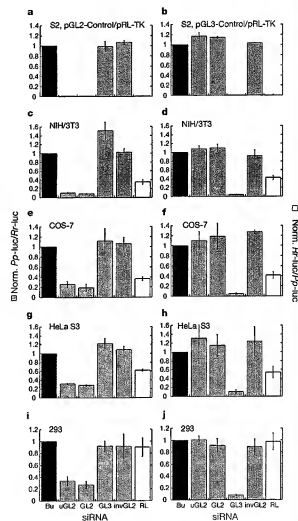


Figure 2 RNA interference by siRNA duplexes. Ratios of target to control luciferase were normalized to a buffer control (Bu, black bars); grey bars indicate ratios of *Photinus pyralis* (*Pp-luc*) GL2 or GL3 luciferase to *Renilla reniformis* (*Rl-luc*) RL luciferase (left axis), white bars indicate RL to GL2 or GL3 ratios (right axis). **a, c, e, g** and **i**, Experiments performed with the combination of pGL2-Control and pRL-TK reporter plasmids; **b, d, f, h** and **j**, experiments performed with the combination of pGL3-Control and pRL-TK reporter plasmids. The cell line used for the interference experiment is indicated at the top of each plot. The ratios of *Pp-luc*/*Rl-luc* for the buffer control (Bu) varied between 0.5 and 10 for pGL2/pRL, and between 0.03 and 1 for pGL3/pRL, respectively, before normalization and between the various cell lines tested. The plotted data were averaged from three independent experiments \pm s.d.

uridine residues. The thymidine overhang was chosen because it reduces costs of RNA synthesis and may enhance nuclease resistance of siRNAs in the cell culture medium and within transfected cells. As in the *Drosophila in vitro* system (data not shown), substitution of uridine by thymidine in the 3' overhang was well tolerated in cultured mammalian cells (Fig. 2a, c, e, g and i), and the sequence of the overhang appears not to contribute to target recognition⁹.

In co-transfection experiments, 25 nM siRNA duplexes were used (Figs 2 and 3; concentration is in respect to the final volume of tissue culture medium). Increasing the siRNA concentration to 100 nM did not enhance the specific silencing effects, but started to affect transfection efficiencies, perhaps due to competition for liposome encapsulation between plasmid DNA and siRNA (data not shown). Decreasing the siRNA concentration to 1.5 nM did not reduce the specific silencing effect (data not shown), even though the siRNAs were now only 2- to 20-fold more concentrated than the DNA plasmids; the silencing effect only vanishes completely if the siRNA concentration was dropped below 0.05 nM. This indicates that siRNAs are extraordinarily powerful reagents for mediating gene silencing, and that siRNAs are effective at concentrations that are several orders of magnitude below the concentrations applied in conventional antisense or ribozyme gene-targeting experiments¹⁹.

To monitor the effect of longer dsRNAs on mammalian cells, 50- and 500-bp dsRNAs that are cognate to the reporter genes were prepared. As a control for nonspecific inhibition, dsRNAs from humanized GFP (hGFP)¹⁹ was used. In these experiments, the reporter plasmids were co-transfected with either 0.21 µg siRNA duplexes or 0.21 µg longer dsRNAs. The siRNA duplexes only reduced the expression of their cognate reporter gene, while the longer dsRNAs strongly and nonspecifically reduced reporter-gene expression. The effects are illustrated for HeLa S3 cells as a representative example (Fig. 3a and b). The absolute luciferase activities were decreased nonspecifically 10- to 20-fold by 50-bp dsRNA, and 20- to 200-fold by 500-bp dsRNA co-transfection, respectively. Similar nonspecific effects were observed for COS-7 and NIH/3T3 cells. For 293 cells, a 10- to 20-fold nonspecific reduction was observed only for 500-bp dsRNAs. Nonspecific reduction in reporter-gene expression by dsRNA > 30 bp was expected as part of the interferon response⁴⁴. Interestingly, superimposed on the nonspecific interferon response, we detect additional sequence-specific, dsRNA-mediated silencing. The sequence-specific silencing effect of long dsRNAs, however, became apparent only when the relative reporter-gene activities were normalized to the hG dsRNA controls (Fig. 3c). Sequence-specific silencing by 50- or 500-bp dsRNAs reduced the targeted reporter-gene expression by an additional 2- to 5-fold. Similar effects were also detected in the other three mammalian cell lines tested (data not shown). Specific silencing effects with dsRNAs (356-1,662 bp) were previously reported in CHO-K1 cells, but the amounts of dsRNA required to detect a 2- to 4-fold specific reduction were about 20-fold higher than in our experiments¹². Also, CHO-K1 cells appear to be deficient in the interferon response. In another report, 293, NIH/3T3 and BHK-21 cells were tested for RNAi using luciferase/β-galactosidase (lacZ) reporter combinations and 829-bp specific lacZ or 717-bp nonspecific green fluorescent protein (GFP) dsRNA¹⁶. The lack of detected RNAi in this case may be due to the less sensitive luciferase/lacZ reporter assay and the length differences of target and control dsRNA. Taken together, our results indicate that RNAi is active in mammalian cells, but that the silencing effect is difficult to detect if the interferon system is activated by dsRNA > 30 bp.

To test for silencing of endogenous genes, we chose four genes coding for cytoskeletal proteins: lamin A/C, lamin B1, nuclear mitotic apparatus protein (NuMA) and vimentin²⁷. The selection was based on the availability of antibodies needed to quantitate the silencing effect. Silencing was monitored 40 to 45 h after transfection to allow for turnover of the protein of the targeted genes. As

shown in Fig. 4, the expression of lamin A/C was specifically reduced by the cognate siRNA duplex (Fig. 4a), but not when nonspecific siRNA directed against firefly luciferase (Fig. 4b) or buffer (Fig. 4c) was used. The expression of a non-targeted gene, NuMA, was unaffected in all treated cells (Fig. 4d-f), demonstrating the integrity of the targeted cells. The reduction in lamin A/C proteins was more than 90% complete as quantified by western blotting (Fig. 4j, k). We note that lamin A/C 'knock-out' mice are

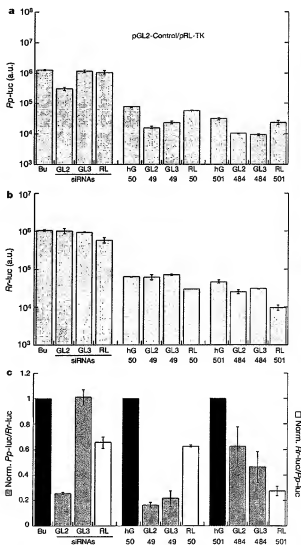


Figure 3 Effects of 21-nucleotide siRNAs, 50-bp, and 500-bp dsRNAs on luciferase expression in HeLa cells. The exact length of the long dsRNAs in base pairs is indicated below the bars. Experiments were performed with pGL2-Control and pRL-TK reporter plasmids. The data were averaged from two independent experiments \pm s.d. a, Absolute Pp-luc expression, plotted in arbitrary luminescence units (a.u.). b, R-luc expression, plotted in arbitrary luminescence units. c, Ratios of normalized target to control luciferase. The ratios of luciferase activity for siRNA duplexes were normalized to a buffer control (Bu, black bars); the luminescence ratios for 50- or 500-bp dsRNAs were normalized to the respective ratios observed for 50- and 500-bp dsRNAs from humanized GFP (hG, black bars). We note that the overall differences in sequence between the 49- and 484-bp GL2 and GL3 dsRNAs are not sufficient to confer specificity for targeting GL2 and GL3 targets (43-nucleotide uninterrupted identity in 49-bp segment, 239-nucleotide longest uninterrupted identity in 484-bp segment³⁹).

viable for a few weeks after birth²⁷ and that the lamin A/C knock-down in cultured cells was not expected to cause cell death. Lamin A and C are produced by alternative splicing in the 3' region and are present in equal amounts in the lamina of mammalian cells (Fig. 4j, k). Transfection of siRNA duplexes targeting lamin B1 and NuMA reduced the expression of these proteins to low levels (data not shown), but we were not able to observe a reduction in vimentin expression. This could be due to the high abundance of vimentin in the cells (several per cent of total cell mass) or because the siRNA sequence chosen was not optimal for targeting vimentin.

The mechanism of the 21-nucleotide siRNA-mediated interference process in mammalian cells remains to be uncovered, and silencing might occur post-transcriptionally and/or transcriptionally. In *Drosophila* lysate, siRNA duplexes mediate post-transcriptional gene silencing by reconstitution of siRNA-protein complexes (siRNPs), which guide mRNA recognition and targeted cleavage^{6,7,9}. In plants, dsRNA-mediated post-transcriptional silencing has also been linked to DNA methylation, which may also be directed by 21-

nucleotide siRNAs²⁴. Methylation of promoter regions can lead to transcriptional silencing²⁵, but methylation in coding sequences does not²⁶. DNA methylation and transcriptional silencing in mammals are well documented processes²⁷, yet their mechanisms have not been linked to that of post-transcriptional silencing. Methylation in mammals is predominantly directed towards CpG dinucleotide sequences. There is no CpG sequence in the RL or lamin A/C siRNA, although both siRNAs mediate specific silencing in mammalian cell culture, so it is unlikely that DNA methylation is essential for the silencing process.

Thus we have shown, for the first time, siRNA-mediated gene silencing in mammalian cells. The use of exogenous 21-nucleotide siRNAs holds great promise for analysis of gene function in human cell culture and the development of gene-specific therapeutics. It will also be of interest in understanding the potential role of endogenous siRNAs in the regulation of mammalian gene function. □

Methods

RNA preparation

21-nucleotide RNAs were chemically synthesized using Expedite RNA phosphoramidites and thymidine phosphoramidite (Frolog, Germany). Synthetic oligonucleotides were deprotected and gel-purified. The accession numbers given here are from GenBank. The siRNA sequences targeting GL2 (Acc. No. 365314) and GL3 luciferase (Acc. No. U47296) corresponded to the coding regions 153–173 relative to the first nucleotide of the start codon; siRNAs targeting RL (Acc. No. AF025846) corresponded to region 119–139 after the start codon. The siRNA sequence targeting lamin A/C (Acc. No. X03444) was from position 608–630 relative to the start codon; lamin B1 (Acc. No. U00057) siRNA was from position 675–694; NuMA (Acc. No. Z11931) siRNA from position 3,968–4,010, and vimentin (Acc. No. NM_003380) from position 346–368 relative to the start codon. Longer RNAs were transcribed with T7 RNA polymerase from polymerase chain reaction (PCR) products, followed by gel purification. The 49- and 484-bp GL2 or GL3 dsRNAs corresponded to positions 113–161 and 113–586, respectively, relative to the start of translation; the 50- and 501-bp RL dsRNAs corresponded to position 118–167 and 118–618, respectively. PCR templates for dsRNA synthesis targeting humanized GFP (hGFP) were amplified from pAD3 (ref. 21), whereby 50- and 501-bp hG dsRNA corresponded to positions 121–170 and 121–631, respectively, to the start codon.

For annealing of siRNAs, 20 µM single strands were incubated in annealing buffer (100 mM potassium acetate, 30 mM HEPES-KOH at pH 7.4, 2 mM magnesium acetate) for 1 min at 90°C followed by 1 h at 37°C. The 37°C incubation step was extended overnight for the 50- and 500-bp dsRNAs, and these annealing reactions were performed at 8.4 µM and 0.84 µM strand concentrations, respectively.

Cell culture

S2 cells were propagated in Schneider's *Drosophila* medium (Life Technologies) supplemented with 10% fetal bovine serum (FBS) (100 units ml⁻¹ penicillin, and 100 µg ml⁻¹ streptomycin) at 25°C. PMA, NuMA, Hela S3, Hela S5, COS-7 cells were grown at 37°C in Dulbecco's modified Eagle's medium supplemented with 10% FBS, 100 units ml⁻¹ penicillin, and 100 µg ml⁻¹ streptomycin. Cells were regularly passaged to maintain exponential growth. Twenty-four hours before transfection at 50–80% confluency, mammalian cells were trypsinized and diluted 1:5 with fresh medium without antibiotics (1–3 × 10⁶ cells ml⁻¹) and transferred to 24-well plates (500 µl per well). S2 cells were not trypsinized before splitting. Co-transfection of reporter plasmids and siRNAs was carried out with Lipofectamine 2000 (Life Technologies) as described by the manufacturer for adherent cell lines. Per well, 1.0 µg pGL2-Control (Promega) or pGL3-Control (Promega), 0.1 µg pTK-Puro (Promega), and 0.21 µg siRNA duplex or dsRNA, formulated into liposomes, were applied; the final volume was 600 µl per well. Cells were incubated 20 h after transfection and appeared healthy thereafter. Luciferase expression was subsequently monitored with the Dual luciferase assay (Promega). Transfection efficiencies were determined by fluorescence microscopy for mammalian cells (luciferase co-transfection of 1.1 µg hGFP-encoding pAD3 (ref. 21) and 0.21 µg inverted GL2 siRNA, and were 70–90%). Reporter plasmids were amplified in XL-1 Blue (Stratagene) and purified using the Qiagen EndoFree Maxi Plasmid Kit.

Transfection of siRNAs for targeting endogenous genes was carried out using Oligofectamine (Life Technologies) and 0.84 µg siRNA duplex per well, but it was recently found that as little as 0.01 µg siRNAs per well are sufficient to mediate silencing. Hela S5 cells were transfected once to three times in approximately 15 h intervals and were assayed 40 to 45 h after the first transfection. It appears, however, that a single transfection is as efficient as multiple transfections. Transfection efficiencies as determined by immunofluorescence of targeted cells were in the range of 90%. Specific silencing of targeted genes was confirmed by at least three independent experiments.

Western blotting and immunofluorescence microscopy

Monoclonal 636 lamin A/C specific antibody²⁸ was used as undiluted hybridoma supernatant for immunofluorescence and 1:100 dilution for western blotting. Affinity-purified polyclonal NuMA protein 705 antibody²⁹ was used at a concentration of 10 µg ml⁻¹ for

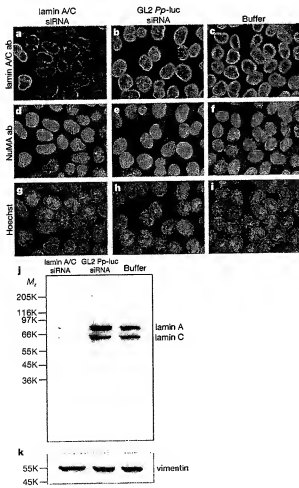


Figure 4 Silencing of nuclear envelope proteins lamin A/C in HeLa cells. Triple fluorescence staining of cells transfected with lamin A/C siRNA duplex (a, d, g), GL2 luciferase siRNA duplex (non-specific siRNA control) (b, e, h), and with buffer only (c, f, i). a–c, Staining with lamin A/C specific antibody; d–f, staining with NuMA-specific antibody; g–i, Hoechst staining of nuclear chromatin. Bright fluorescent nuclei in a represent untransfected cells. j, k, Western blots of transfected cells using lamin A/C (j) or vimentin-specific (k) antibodies. The Western blot was stripped and re-probed with vimentin antibody to check for equal loading of total protein.

immunofluorescence. Monoclonal V9 vimentin-specific antibody was used at 1/2,000 dilution. For western blotting, transfected cells grown in 24-well plates were trypsinized and harvested in SDS sample buffer. Equal amounts of total protein were separated on 12.5% polyacrylamide gels and transferred to nitrocellulose. Standard immunostaining was carried out using ECL enhanced chemiluminescence technique (Amersham Pharmacia).

For immunofluorescence, transfected cells grown on glass coverslips in 24-well plates were fixed in methanol for 6 min at -10°C . Target gene specific and control primary antibody were added and incubated for 80 min at 37°C . After washing in phosphate buffered saline (PBS), Alexa 488-conjugated anti-rabbit (Molecular Probes) and Cy3-conjugated anti-mouse (Dianova) antibodies were added and incubated for 60 min at 37°C . Finally, cells were stained for 4 min at room temperature with Hoechst 33342 (1 μM in PBS) and embedded in Mowiol 488 (Hoechst). Pictures were taken using a Zeiss AxioPhot camera with a Fluor 40X/1.30 oil objective and MetaMorph Imaging Software (Universal Imaging Corporation) with equal exposure times for the specific antibodies.

Received 20 February; accepted 26 April 2001.

- Fire, A. RNA-triggered gene silencing. *Trends Genet.* **15**, 358–363 (1999).
- Sharp, P. A. RNA interference 2001. *Genes Dev.* **15**, 485–490 (2001).
- Hannon, S. M., Coudy, A. A. & Hanson, G. J. Post-transcriptional gene silencing by double-stranded RNA. *Nature Rev. Genet.* **2**, 110–119 (2001).
- Tuschli, T. RNA interference and small interfering RNAs. *Chem. Biotechnol.* **2**, 239–245 (2001).
- Hamilton, A. J. & Balcomb, D. C. A species of small RNA in posttranscriptional gene silencing in plants. *Science* **286**, 950–952 (1999).
- Hannon, S. M., Bernatchez, L., Birch, D. & Hanson, G. J. An RNA-directed nuclease mediates post-transcriptional gene silencing in *Drosophila* cells. *Nature* **404**, 293–296 (2000).
- Zamore, P. D., Tuschli, T., Sharp, P. A. & Bartel, D. P. RNAi: Double-stranded RNA directs the ATP-dependent cleavage of mRNA at 21 to 23 nucleotide intervals. *Cell* **101**, 25–33 (2000).
- Bernatchez, L., Coudy, A. A., Hannon, S. M. & Hanson, G. J. Role for a bifunctional ribonuclease in the initiation step of RNA interference. *Nature* **409**, 348–353 (2001).
- Espenshott, S. M., Lendeckel, W. & Tuschli, T. RNA interference is mediated by 21 and 22 nt RNAs. *Genes Dev.* **15**, 188–200 (2001).
- Capien, N. J., Frenois, J., Fire, A. & Morgan, R. A. dsRNA-mediated gene silencing in cultured *Drosophila* cells: a tissue culture model for the analysis of RNA interference. *Genes Dev.* **15**, 100–108 (2000).
- Clemens, J. C. et al. Use of double-stranded RNA interference in *Drosophila* cell lines to disrupt signal transduction pathways. *Proc. Natl. Acad. Sci. USA* **97**, 6499–6503 (2000).
- Li, T.-S. K., Zeng, S., Miyata, Y. & Saigo, K. Sensitive assay of RNA interference in *Drosophila* and Chinese hamster cultured cells using firefly luciferase gene as target. *FEBS Lett.* **479**, 79–82 (2000).
- Wianney, F. & Zernicke-Otzu, M. Specific interference with gene function by double-stranded RNA in early mouse development. *Nature Cell Biol.* **2**, 70–75 (2000).
- Brubaker, F., Stein, R., Hayashi, H. & Schuler, R. M. Selective acquisition of dormant maternal mRNA in mouse oocytes by RNA interference. *Development* **127**, 4147–4156 (2000).
- Buhrman, M. B. & Zarh, H. Transcriptional silencing of rodent riboprotein (r) collagen by a homologous transcriptionally self-induced nuclease. *Mol. Cell Biol.* **19**, 274–288 (1999).
- Stack, G. R., Kren, L. M., Williams, B. R., Stevenson, R. H. & Scheraga, R. D. How cells respond to interferons. *Annu. Rev. Biochem.* **69**, 227–264 (1998).
- Jahneke, L., Green, S. R., Schmidt, C. & Mathews, M. B. Interactions between double-stranded RNA regulators and the protein kinase DAI. *Mol. Cell Biol.* **12**, 5238–5248 (1992).
- Mink, A. A., West, D. K., Benoit, S. & Baglioni, C. Structural requirements of double-stranded RNA for the activation of 2',5'-oligoadenylate polymerase and protein kinase of interferon-treated HeLa cells. *J. Biol. Chem.* **254**, 10188–10193 (1979).
- Clemens, M. & Williams, B. Inhibition of cell-free protein synthesis by ppvA⁺ pA⁺ pA⁺: a novel oligonucleotide synthesized by interferon-treated L cell extracts. *Cell* **13**, 563–572 (1978).
- Majumder, D. G. et al. Inhibition of hepatitis C virus (HCV)-dependent translation and replication of a chimeric HCV poliovirus using synthetic double-stranded ribozymes. *Hepatology* **31**, 769–776 (2000).
- Kehlenbock, R. H., Dickmanns, A. & Gerson, L. Nucleocytoplasmic shuttling factors including Ran and CRM1 mediate nuclear export of NFAT in virus. *J. Cell Biol.* **141**, 663–674 (1998).
- Kren, T. & Vils, R. *Guidelines for the Crystallographic and Mass Spectroscopic Data Bank* (Oxford University Press, Oxford, 1999).
- Sullivan, T. et al. Loss of A-type tRNA expression compromises nuclear envelope integrity leading to muscular dystrophy. *J. Cell Biol.* **147**, 913–920 (1999).
- Vasquez, R. M. RNA-directed DNA methylation. *Plant Mol. Biol.* **43**, 203–209 (2000).
- Meyer, M. F., Adkins, W., van der Vliet, J., Mink, M. A. & Mathews, A. J. M. Transcriptional silencing and promoter methylation triggered by double-stranded RNA. *EMBO J.* **19**, 5194–5201 (2000).
- Yang, M.-B., Wesley, S. V., Finnegan, E. J., Smith, N. A. & Waterhouse, P. M. Replicating satellite RNA induces sequence-specific DNA methylation and transcribed transcripts in plants. *RNA* **5**, 16–28 (1997).
- Rizov, A. CpG methylation, chromatin structure and gene silencing—a three-way connection. *EMBO J.* **17**, 4905–4908 (1998).
- Roberts, R. A., Giesler, R. K., Peters, J. H., Weber, K. & Osborn, M. Induction of nuclear lamina A/C in macrophages in *in vivo* cultures of rat bone marrow precursor cells and human blood monocytes, and in macrophages elicited *in vivo* by thymicallike stimulation. *Exp. Cell Res.* **180**, 185–194 (1990).
- Harborth, J., Wang, J., Gullen-Hall, C., Weber, K. & Osborn, M. Self assembly of Na⁺/magnesium oligomers as structural units of a nuclear lattice. *EMBO J.* **15**, 1689–1700 (1999).
- Parish, S., Frenois, J., Xu, S., Helt, A. & Fire, A. Functional anatomy of a dsRNA trigger: Differential requirement for the two trigger strands in RNA interference. *Mol. Cell* **6**, 1077–1087 (2000).

Acknowledgements

We thank J. Martinez, J. Ludwig and D. Bortel for comments on the manuscript; J. Prodel for help with image processing; H.-J. Dehne for technical assistance; F. Döring, R. Niehning,

D. Ingelfinger and C. Schneider for supplying cell lines; A. Dickmanns for the gift of the plasmid pAD3; and R. Lehmann for support. This work was funded by a BioFuture grant of the Bundesministerium für Bildung und Forschung.

Correspondence and requests for materials should be addressed to T.T. (e-mail: ttuschli@mpipbc.gwdg.de).

Ribosomal peptidyl transferase can withstand mutations at the putative catalytic nucleotide

Norbert Polacek, Marne Gayner, Aymen Yassin & Alexander S. Mankin

Center for Pharmaceutical Biotechnology (MC 870), University of Illinois, 900 South Ashland Avenue, Chicago, Illinois 60607, USA

Peptide bond formation is the principal reaction of protein synthesis. It takes place in the peptidyl transferase centre of the large (50S) ribosomal subunit. In the course of the reaction, the polypeptide is transferred from peptidyl transfer RNA to the α -amino group of amino acyl-tRNA. The crystallographic structure of the 50S subunit showed no proteins within 18 Å from the active site, revealing peptidyl transferase as an RNA enzyme¹. Reported unique structural and biochemical features of the universally conserved adenine residue A2451 in 23S ribosomal RNA (*Escherichia coli* numbering) led to the proposal of a mechanism of rRNA catalysis that implicates this nucleotide as the principal catalytic residue^{2,3}. *In vitro* genetics allowed us to test the importance of A2451 for the overall rate of peptide bond formation. Here we report that large ribosomal subunits with mutated A2451 showed significant peptidyl transferase activity in several independent assays. Mutations at another nucleotide, G2447, which is essential to render catalytic properties to A2451 (refs 2, 3), also did not dramatically change the transpeptidation activity. As alterations of the putative catalytic residues do not severely affect the rate of peptidyl transfer the ribosome apparently promotes transpeptidation not through chemical catalysis, but by properly positioning the substrates of protein synthesis. The proposed role of A2451 in the peptidyl transfer reaction is

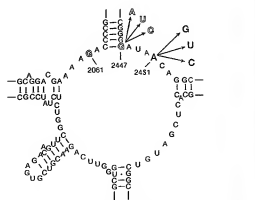


Figure 1 The secondary structure of the central loop of domain V of *T. aquaticus* 23S rRNA. Position A2451 (*E. coli* 23S rRNA numbering), the principal catalytic nucleotide in the proposed general acid–base catalytic mechanism of peptide bond formation³, is shown in bold. Its tertiary interaction partners, guanine residues 2061 and 2447, suggested to be essential for rendering catalytic properties to A2451, are outlined. Arrows indicate the mutations engineered in 23S rRNA.